PHYSICAL REVIEW D **89,** 032001 (2014)

Studies of beauty baryon decays to D^0ph^- and $\Lambda_c^+h^-$ final states

R. Aaij *et al.**
(LHCb Collaboration)

(Received 20 November 2013; published 13 February 2014)

Decays of beauty baryons to the D^0ph^- and $\Lambda_c^+h^-$ final states (where h indicates a pion or a kaon) are studied using a data sample of pp collisions, corresponding to an integrated luminosity of 1.0 fb^{-1}, collected by the LHCb detector. The Cabibbo-suppressed decays $\Lambda_b^0 \to D^0pK^-$ and $\Lambda_b^0 \to \Lambda_c^+K^-$ are observed, and their branching fractions are measured with respect to the decays $\Lambda_b^0 \to D^0p\pi^-$ and $\Lambda_b^0 \to \Lambda_c^+\pi^-$. In addition, the first observation is reported of the decay of the neutral beauty-strange baryon Ξ_b^0 to the D^0pK^- final state, and a measurement of the Ξ_b^0 mass is performed. Evidence of the $\Xi_b^0 \to \Lambda_c^+K^-$ decay is also reported.

DOI: 10.1103/PhysRevD.89.032001 PACS numbers: 14.20.Mr, 13.30.Eg, 14.20.−c

I. INTRODUCTION

Although there has been great progress in studies of beauty mesons, both at the B factories and hadron machines, the beauty baryon sector remains largely unexplored. The quark model predicts seven ground-state ($J^P = \frac{1}{2}^+$) baryons involving a b quark and two light (u, d, or s) quarks [1]. These are the Λ_b^0 isospin singlet, the Σ_b triplet, the Ξ_b strange doublet, and the doubly strange state Ω_b^-. Among these states, the Σ_b^0 baryon has not been observed yet, while for the others the quantum numbers have not been experimentally established, very few decay modes have been measured, and fundamental properties such as masses and lifetimes are in general poorly known. Moreover, the $\Sigma_b^\pm$ and Ξ_b^0 baryons have been observed by a single experiment [2,3]. It is therefore of great interest to study b baryons and to determine their properties.

The decays of b baryons can be used to study CP violation and rare processes. In particular, the decay $\Lambda_b^0 \to D^0\Lambda$ has been proposed to measure the Cabibbo–Kobayashi–Maskawa unitarity triangle angle γ [4–6], following an approach analogous to that for $B^0 \to DK^{*0}$ decays [7]. A possible extension to the analysis of the $D^0\Lambda$ final state is to use the $\Lambda_b^0 \to D^0pK^-$ decay, with the pK^- pair originating from the Λ_b^0 decay vertex. Such an approach can avoid limitations due to the lower reconstruction efficiency of the Λ decay. In addition, if the full phase space of the three-body decay is used, the sensitivity to γ may be enhanced, in a similar manner to the Dalitz plot analysis of $B^0 \to DK^+\pi^-$ decays, which offers certain advantages over the quasi-two-body $B^0 \to DK^{*0}$ analysis [8,9].

This paper reports the results of a study of beauty baryon decays into $D^0p\pi^-$, D^0pK^-, $\Lambda_c^+\pi^-$, and $\Lambda_c^+K^-$ final states.[1] A data sample corresponding to an integrated luminosity of 1.0 fb^{-1} is used, collected by the LHCb detector [10] in pp collisions with center-of-mass energy of 7 TeV. Six measurements are performed in this analysis, listed below.[1]

The decay mode $\Lambda_b^0 \to D^0p\pi^-$ is the Cabibbo-favored partner of $\Lambda_b^0 \to D^0pK^-$ with the same topology and higher rate. We measure its rate using the mode $\Lambda_b^0 \to \Lambda_c^+\pi^-$ for normalization. To avoid dependence on the poorly measured branching fraction of the $\Lambda_c^+ \to pK^-\pi^+$ decay, we quote the ratio

$$R_{\Lambda_b^0\to D^0p\pi^-} \equiv \frac{\mathcal{B}(\Lambda_b^0 \to D^0p\pi^-) \times \mathcal{B}(D^0 \to K^-\pi^+)}{\mathcal{B}(\Lambda_b^0 \to \Lambda_c^+\pi^-) \times \mathcal{B}(\Lambda_c^+ \to pK^-\pi^+)}. \quad (1)$$

The D^0 meson is reconstructed in the favored final state $K^-\pi^+$ and the Λ_c^+ baryon in the $pK^-\pi^+$ mode. In this way, the $\Lambda_b^0 \to \Lambda_c^+\pi^-$ and $\Lambda_b^0 \to D^0p\pi^-$ decays have the same final state particles, and some of the systematic uncertainties, in particular those related to particle identification (PID), cancel in the ratio. The branching fraction of the Cabibbo-suppressed $\Lambda_b^0 \to D^0pK^-$ decay mode is measured with respect to that of $\Lambda_b^0 \to D^0p\pi^-$:

$$R_{\Lambda_b^0\to D^0pK^-} \equiv \frac{\mathcal{B}(\Lambda_b^0 \to D^0pK^-)}{\mathcal{B}(\Lambda_b^0 \to D^0p\pi^-)}. \quad (2)$$

The Cabibbo-suppressed decay $\Lambda_b^0 \to \Lambda_c^+K^-$ is also studied. This decay has been considered in various analyses as a background component [11,12], but a dedicated study has not been performed so far. We measure the ratio

$$R_{\Lambda_b^0\to \Lambda_c^+K^-} \equiv \frac{\mathcal{B}(\Lambda_b^0 \to \Lambda_c^+K^-)}{\mathcal{B}(\Lambda_b^0 \to \Lambda_c^+\pi^-)}. \quad (3)$$

* Full author list given at the end of the article.

[1]The inclusion of the charge-conjugate processes is implied.

The heavier beauty-strange Ξ_b^0 baryon can also decay into the final states D^0pK^- and $\Lambda_c^+K^-$ via $b \to c\bar{u}d$ color-suppressed transitions. Previously, the Ξ_b^0 baryon has only been observed in one decay mode, $\Xi_b^0 \to \Xi_c^+\pi^-$ [3]; thus, it is interesting to study other final states, as well as to measure its mass more precisely. Here we report measurements of the ratios of rates for $\Xi_b^0 \to D^0pK^-$,

$$R_{\Xi_b^0 \to D^0pK^-} \equiv \frac{f_{\Xi_b^0} \times \mathcal{B}(\Xi_b^0 \to D^0pK^-)}{f_{\Lambda_b^0} \times \mathcal{B}(\Lambda_b^0 \to D^0pK^-)}, \quad (4)$$

and $\Xi_b^0 \to \Lambda_c^+K^-$ decays,

$$R_{\Xi_b^0 \to \Lambda_c^+K^-} \equiv \frac{\mathcal{B}(\Xi_b^0 \to \Lambda_c^+K^-) \times \mathcal{B}(\Lambda_c^+ \to pK^-\pi^+)}{\mathcal{B}(\Xi_b^0 \to D^0pK^-) \times \mathcal{B}(D^0 \to K^-\pi^+)}, \quad (5)$$

where $f_{\Xi_b^0}$ and $f_{\Lambda_b^0}$ are the fragmentation fractions of the b quark to Ξ_b^0 and Λ_b^0 baryons, respectively. The difference of Ξ_b^0 and Λ_b^0 masses, $m_{\Xi_b^0} - m_{\Lambda_b^0}$, is also measured.

II. DETECTOR DESCRIPTION

The LHCb detector [10] is a single-arm forward spectrometer covering the pseudorapidity range $2 < \eta < 5$, designed for the study of particles containing b or c quarks. The detector includes a high-precision tracking system consisting of a silicon-strip vertex detector surrounding the pp interaction region, a large-area silicon-strip detector located upstream of a dipole magnet with a bending power of about 4 Tm, and three stations of silicon-strip detectors and straw drift tubes placed downstream. The combined tracking system provides a momentum measurement with relative uncertainty that varies from 0.4% at 5 GeV/c to 0.6% at 100 GeV/c and impact parameter (IP) resolution of 20 μm for tracks with high transverse momentum (p_T). Charged hadrons are identified using two ring-imaging Cherenkov (RICH) detectors [13]. Photon, electron, and hadron candidates are identified by a calorimeter system consisting of scintillating-pad and preshower detectors, an electromagnetic calorimeter, and a hadronic calorimeter. Muons are identified by a system composed of alternating layers of iron and multiwire proportional chambers [14].

The trigger [15] consists of a hardware stage, based on information from the calorimeter and muon systems, followed by a software stage, which applies a full event reconstruction. Events used in this analysis are required to satisfy at least one hardware trigger requirement: a final-state particle has to deposit energy in the calorimeter system above a certain threshold, or the event has to be triggered by any of the requirements not involving the signal decay products. The software trigger requires a two-, three-, or four-track secondary vertex with a high sum of p_T of the tracks and a significant displacement from the primary pp interaction vertices (PVs). At least one track should have $p_T > 1.7$ GeV/c and χ^2_{IP} with respect to any PV greater than 16, where χ^2_{IP} is defined as the difference in χ^2 of a given PV reconstructed with and without the considered track. A multivariate algorithm [16] is used for the identification of secondary vertices consistent with the decay of a b hadron.

In the simulation, pp collisions are generated using PYTHIA 6.4 [17] with a specific LHCb configuration [18]. Decays of hadronic particles are described by EVTGEN [19]; the interaction of the generated particles with the detector and its response are implemented using the GEANT4 toolkit [20,21] as described in Ref. [22].

III. SELECTION CRITERIA

The analysis uses four combinations of final-state particles to form the b-baryon candidates: $\Lambda_c^+\pi^-$, $D^0p\pi^-$, $\Lambda_c^+K^-$, and D^0pK^-. The D^0 mesons are reconstructed in the $K^-\pi^+$ final state, and Λ_c^+ baryons are reconstructed from $pK^-\pi^+$ combinations. In addition, the combinations with the D^0 meson of opposite flavor (i.e., $\bar{D}^0p\pi^-$ and $\bar{D}^0pK^-$ with $\bar{D}^0 \to K^+\pi^-$) are selected to better constrain the shape of the combinatorial background in D^0ph^- final states. These decay modes correspond to either doubly Cabibbo-suppressed decays of the D^0, or to $b \to u$ transitions in the Λ_b^0 and Ξ_b^0 decays, and are expected to contribute a negligible amount of signal in the current data sample.

The selection of b-baryon candidates is performed in two stages: the preselection and the final selection. The preselection is performed to select events containing a beauty hadron candidate with an intermediate charm state. It requires that the tracks forming the candidate, as well as the beauty and charm vertices, have good quality and are well separated from any PV, and the invariant masses of the beauty and charm hadrons are in the region of the known values of the masses of the corresponding particles. The preselection has an efficiency of 95%–99% for the signal depending on the decay mode.

Two different sets of requirements are used for the final selection. The ratio $R_{\Lambda_b^0 \to D^0p\pi^-}$ is measured by fitting the invariant mass distribution for candidates obtained with a *loose* selection to minimize the systematic uncertainty. The signal yields of these decays are large, and the uncertainty in the ratio is dominated by systematic effects. The ratios $R_{\Lambda_b^0 \to D^0pK^-}$ and $R_{\Lambda_b^0 \to \Lambda_c^+K^-}$ are less affected by systematic uncertainties since the topologies of the decays are the same. A *tight* multivariate selection is used in addition to the loose selection requirements when measuring these ratios, as well as the ratios of the Ξ_b^0 decay rates.

The loose selection requires that the invariant masses of the intermediate Λ_c^+ and D^0 candidates are within 25 MeV/c^2 of their known masses [1], and the decay time significance of the D^0 meson from the $\Lambda_b^0 \to D^0p\pi^-$

decay is greater than one standard deviation. The decay time significance is defined as the measured decay time divided by its uncertainty for a given candidate. The final-state particles are required to satisfy PID criteria based on information from the RICH detectors [13]. Pion candidates are required to have a value $\mathrm{DLL}_{K\pi} < 5$ for the difference of logarithms of likelihoods between the kaon and pion hypotheses; the efficiency of this requirement is about 95%. The requirement for kaon candidates of $\mathrm{DLL}_{K\pi} > 0$ is about 97% efficient. The protons are required to satisfy $\mathrm{DLL}_{p\pi} > 5$ and $\mathrm{DLL}_{pK} > 0$. The corresponding efficiency is approximately 88%. The momentum of each final-state track is required to be less than 100 GeV/c, corresponding to the range of good separation between particle types.

For candidates passing the above selections, a kinematic fit is performed [23]. The fit employs constraints on the decay products of the Λ_b^0, Λ_c^+, and D^0 particles to originate from their respective vertices, the Λ_b^0 candidate to originate from the PV, and the Λ_c^+ and D^0 invariant masses to be equal to their known values [1]. A momentum scale correction is applied in the kinematic fit to improve the mass measurement as described in Ref. [24]. The momentum scale of the detector has been calibrated using inclusive $J/\psi \to \mu^+\mu^-$ decays to account for the relative momentum scale between different data taking periods, while the absolute calibration is performed with $B^+ \to J/\psi K^+$ decays.

The tight selection is based on a boosted decision tree (BDT) [25] trained with the gradient boost algorithm. The D^0ph^- selection is optimized using simulated D^0pK^- signal events and combinations with opposite-flavor D^0 candidates ($\bar{D}^0pK^-$) in data as a background estimate. The optimization of the $\Lambda_c^+h^-$ selection is performed with a similar approach, with the $\Lambda_c^+K^+$ candidates as the background training sample. The optimization criteria for the BDTs are the maximum expected statistical significances of the $\Lambda_b^0 \to D^0pK^-$ and $\Lambda_b^0 \to \Lambda_c^+K^-$ signals, $S_{\mathrm{stat}} = N_{\mathrm{sig}}/\sqrt{N_{\mathrm{sig}} + N_{\mathrm{bck}}}$, where N_{sig} and N_{bck} are the expected numbers of signal and background events. The expected number of events for the optimization is taken from the observed yields in the $\Lambda_b^0 \to \Lambda_c^+\pi^-$ and $\Lambda_b^0 \to D^0p\pi^-$ modes scaled by the Cabibbo-suppression factor. The variables that enter the BDT selection are the following: the quality of the kinematic fit (χ^2_{fit}/ndf, where ndf is the number of degrees of freedom in the fit); the minimum IP significance χ^2_{IP} of the final-state and intermediate charm particles with respect to any PV; the lifetime significances of the Λ_b^0 and intermediate charm particles; and the PID variables ($\mathrm{DLL}_{p\pi}$ and DLL_{pK}) for the proton candidate. The D^0ph^- selection has a signal efficiency of 72% on candidates passing the loose selection while retaining 11% of the combinatorial background. The $\Lambda_c^+h^-$ selection is 99.5% efficient and retains 65% of the combinatorial background.

In approximately 2% of events, more than one candidate passes the selection. In these cases, only the candidate with the minimum χ^2_{fit}/ndf is retained for further analysis.

Several vetoes are applied for both the loose and tight selections to reduce backgrounds. To veto candidates formed from $J/\psi \to \mu^+\mu^-$ combined with two tracks, at least one of the pion candidates in $\Lambda_c^+\pi^-$ and $D^0p\pi^-$ combinations is required not to have hits in the muon chambers. For D^0ph^- combinations, a $\Lambda_c^+ \to p\pi^+h^-$ veto is applied: the invariant mass of the $p\pi^+h^-$ combination is required to differ from the nominal Λ_c^+ mass by more than 20 MeV/c^2. This requirement rejects the background from $\Lambda_b^0 \to \Lambda_c^+K^-$ decays. Cross-feed between $\Lambda_b^0 \to D^0ph^-$ and $\Lambda_b^0 \to \Lambda_c^+\pi^-$ decays does not occur since the invariant mass of the D^0p combination in $\Lambda_b^0 \to D^0ph^-$ decays is greater than the Λ_c^+ invariant mass.

IV. DETERMINATION OF SIGNAL YIELDS

The signal yields are obtained from extended maximum likelihood fits to the unbinned invariant mass distributions. The fit model includes signal components (Λ_b^0 only for $\Lambda_c^+\pi^-$ and $D^0p\pi^-$ final states and both Λ_b^0 and Ξ_b^0 for D^0pK^- and $\Lambda_c^+K^-$ final states) as well as various background contributions. The ratio $R_{\Lambda_b^0 \to D^0p\pi^-}$ is obtained from the combined fit of the $\Lambda_c^+\pi^-$ and $D^0p\pi^-$ invariant mass distributions of candidates that pass the loose selection, while the other quantities are determined from the simultaneous fit of the $\Lambda_c^+h^-$, D^0ph^-, and $\bar{D}^0ph^-$ ($h = \pi$ or K) invariant mass distributions passing the tight BDT-based selection requirements.

The shape of each signal contribution is taken from simulation and is parametrized using the sum of two Crystal Ball (CB) functions [26]. In the fit to data, the widths of each signal component are multiplied by a common scaling factor that is left free. This accounts for the difference between the invariant mass resolution observed in data and simulation. The masses of the Λ_b^0 and Ξ_b^0 states are also free parameters. Their mean values as reconstructed in the D^0ph^- and $\Lambda_c^+h^-$ spectra are allowed to differ by an amount ΔM (which is the same for Λ_b^0 and Ξ_b^0 masses) to account for possible imperfect calibration of the momentum scale in the detector. The mass difference ΔM obtained from the fit is consistent with zero.

The background components considered in the analysis are subdivided into three classes: random combinations of tracks, or genuine D^0 or Λ_c^+ decays combined with random tracks (combinatorial background); decays where one or more particles are incorrectly identified (misidentification background); and decays where one or more particles are not reconstructed (partially reconstructed background).

The combinatorial background is parametrized with a quadratic function. The shapes are constrained to be the

same for the D^0ph^- signal and $\bar{D}^0ph^-$ background combinations. The $\bar{D}^0p\pi^-$ fit model includes only the combinatorial background component, while in the $\bar{D}^0pK^-$ model, the $\Lambda_b^0 \to \bar{D}^0pK^-$ signal and partially reconstructed background are included with varying yields to avoid biasing the combinatorial background shape. The two contributions are found to be consistent with zero, as expected.

Contributions of charmed B decays with misidentified particles are studied using simulated samples. The $\bar{B}_s^0 \to D_s^+h^-$ and $\bar{B}^0 \to D^+h^-$ decay modes are considered as $\Lambda_c^+h^-$ backgrounds, while $\bar{B}^0 \to D^0\pi^+\pi^-$, $\bar{B}^0 \to D^0K^+K^-$ [27], and $\bar{B}_s^0 \to D^0K^+\pi^-$ [28] are possible backgrounds in the D^0ph^- spectra. These contributions to D^0ph^- modes are found to be negligible and thus are not included in the fit model, while the $\bar{B}_{(s)}^0 \to D_{(s)}^+\pi^-$ component is significant and is included in the fit. The ratio between $\bar{B}_s^0 \to D_s^+\pi^-$ and $\bar{B}^0 \to D^+\pi^-$ contributions is fixed from the measured ratio of their event yields [29].

Contributions to D^0pK^- and $\Lambda_c^+K^-$ spectra from the $\Lambda_b^0 \to D^0p\pi^-$ and $\Lambda_b^0 \to \Lambda_c^+\pi^-$ modes, respectively, with the pion misidentified as a kaon (K/π misidentification backgrounds) are obtained by parametrizing the simulated samples with a CB function. In the case of the $\Lambda_b^0 \to D^0p\pi^-$ background, the squared invariant mass of the D^0p combination, $M^2(D^0p)$, is required to be smaller than 10 GeV$^2/c^4$. This accounts for the dominance of events with low D^0p invariant masses observed in data. In the case of the $\Lambda_c^+\pi^-$ spectrum, the $\Lambda_b^0 \to \Lambda_c^+K^-$ contribution with the kaon misidentified as a pion is also included. In all cases, the nominal selection requirements, including those for PID, are applied to the simulated samples.

Partially reconstructed backgrounds, such as $\Lambda_b^0 \to D^{*0}p\pi^-$, $D^{*0} \to D^0\pi^0/\gamma$ decays, or $\Lambda_b^0 \to \Sigma_c^+\pi^-$, $\Sigma_c^+ \to \Lambda_c^+\pi^0$ decays, contribute at low invariant mass. Simulation is used to check that these backgrounds are well separated from the signal region. However, their mass distribution is expected to depend strongly on the unknown helicity structure of these decays. Therefore, an empirical probability density function (PDF), a bifurcated Gaussian distribution with free parameters, is used to parametrize them. The shapes of the backgrounds are constrained to be the same for the D^0pK^- and $D^0p\pi^-$ decay modes as well as for the $\Lambda_c^+K^-$ and $\Lambda_c^+\pi^-$ decay modes.

Backgrounds from partially reconstructed $\Lambda_b^0 \to D^{*0}p\pi^-$ and $\Lambda_b^0 \to \Sigma_c^+\pi^-$ decays with the pion misidentified as a kaon contribute to the D^0pK^- and $\Lambda_c^+K^-$ mass spectra, respectively. These backgrounds are parametrized with CB functions fitted to samples simulated assuming that the amplitude is constant across the phase space. Their yields are constrained from the yields of partially reconstructed components in the $D^0p\pi^-$ and $\Lambda_c^+\pi^-$ spectra taking into account the K/π misidentification probability.

Charmless $\Lambda_b^0 \to pK^-\pi^+h^-$ backgrounds, which have the same final state as the signal modes but no intermediate charm vertex, are studied with the Λ_b^0 invariant mass fit to data from the sidebands of the $D^0 \to K^-\pi^+$ invariant mass distribution: $50 < |M(K^-\pi^+) - m_{D^0}| < 100$ MeV$/c^2$. Similar sidebands are used in the $\Lambda_c^+ \to pK^-\pi^+$ invariant mass. A significant contribution is observed in the $D^0p\pi^-$ mode. Hence, for the D^0ph^- combinations, the D^0 vertex is required to be downstream of Λ_b^0 vertex, and the D^0 decay time must differ from zero by more than one standard deviation. The remaining contribution is estimated from the Λ_b^0 invariant mass fit in the sidebands. The $\Lambda_b^0 \to D^0p\pi^-$ yield obtained from the fit is corrected for a small residual charmless contribution, while in other modes the contribution of this background is consistent with zero.

The $\Lambda_c^+\pi^-$ and $D^0p\pi^-$ invariant mass distributions obtained with the loose selection are shown in Fig. 1 with the fit result overlaid. The Λ_b^0 yields obtained from the fit to these spectra are presented in Table I. Figures 2 and 3 show

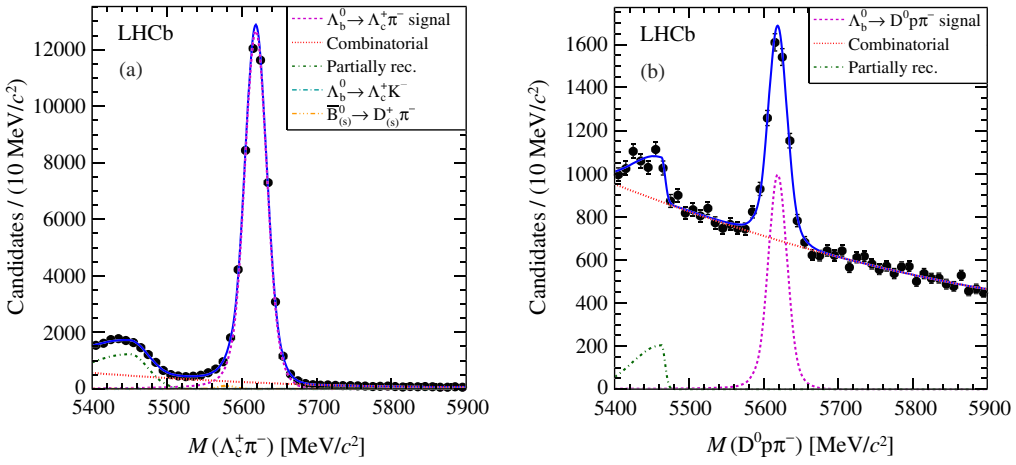

FIG. 1 (color online). Distributions of invariant mass for (a) $\Lambda_c^+\pi^-$ and (b) $D^0p\pi^-$ candidates passing the loose selection (points with error bars) and results of the fit (solid line). The signal and background contributions are shown.

TABLE I. Results of the fit to the invariant mass distribution of $\Lambda_b^0 \to \Lambda_c^+ \pi^-$ and $\Lambda_b^0 \to D^0 p\pi^-$ candidates passing the loose selection. The uncertainties are statistical only.

Decay mode	Yield
$\Lambda_b^0 \to D^0 p\pi^-$	3383 ± 94
$\Lambda_b^0 \to \Lambda_c^+ \pi^-$	$50\,301 \pm 253$

the invariant mass distributions for the $D^0 ph^-$ and $\Lambda_c^+ h^-$ modes after the tight BDT-based selection. The Λ_b^0 and Ξ_b^0 yields, as well as their masses, obtained from the fit are given in Table II. The raw masses obtained in the fit are used to calculate the difference of Ξ_b^0 and Λ_b^0 masses, $m_{\Xi_b^0} - m_{\Lambda_b^0} = 174.8 \pm 2.3\ \mathrm{MeV}/c^2$, which is less affected by the systematic uncertainty due to knowledge of the absolute mass scale.

Figures 4 and 5 show the Dalitz plot of the three-body decay $\Lambda_b^0 \to D^0 p\pi^-$ and the projections of the two invariant masses, where resonant contributions are expected. In the projections, the background is subtracted using the *sPlot* technique [30]. The distributions show an increased density of events in the low $M(D^0 p)$ region, where a contribution from excited Λ_c^+ states is expected. The $\Lambda_c(2880)^+$ state is apparent in this projection. Structures in the $p\pi^-$ combinations are also visible. The Dalitz plot and projections of $D^0 p$ and pK^- invariant masses for the $\Lambda_b^0 \to D^0 pK^-$ mode are shown in Fig. 6. The distributions for the $\Lambda_b^0 \to D^0 pK^-$ mode exhibit similar behavior with the dominance of a low $M(D^0 p)$ contribution and an enhancement in the low $M(pK^-)$ region.

V. CALCULATION OF BRANCHING FRACTIONS

The ratios of branching fractions are calculated from the ratios of yields of the corresponding decays after applying several correction factors,

$$R = \frac{N^i}{N^j} \frac{\varepsilon^j_{\mathrm{sel}}}{\varepsilon^i_{\mathrm{sel}}} \frac{\varepsilon^j_{\mathrm{PID}}}{\varepsilon^i_{\mathrm{PID}}} \frac{\varepsilon^j_{\mathrm{PS}}}{\varepsilon^i_{\mathrm{PS}}}, \tag{6}$$

where N^i is the yield for the ith decay mode, $\varepsilon^i_{\mathrm{sel}}$ is its selection efficiency excluding the PID efficiency, $\varepsilon^i_{\mathrm{PID}}$ is the efficiency of the PID requirements, and $\varepsilon^i_{\mathrm{PS}}$ is the phase-space acceptance correction defined below.

The trigger, preselection, and final selection efficiencies that enter $\varepsilon_{\mathrm{sel}}$ are obtained using simulated signal samples. The selection efficiency is calculated without the PID requirements applied, except for the proton PID in the tight selection, which enters the multivariate discriminant. Since the multiplicities of all the final states are the same, and the kinematic distributions of the decay products are similar, the uncertainties in the efficiencies largely cancel in the quoted ratios of branching fractions.

The efficiencies of PID requirements for kaons and pions are obtained with a data-driven procedure using a large sample of $D^{*+} \to D^0 \pi^+$, $D^0 \to K^-\pi^+$ decays. The calibration sample is weighted to reproduce the kinematic properties of the decays under study taken from simulation.

For protons, however, the available calibration sample $\Lambda \to p\pi^-$ does not cover the full range in momentum-pseudorapidity space that the protons from the signal decays populate. Thus, in the case of the calculation of the ratio of $\Lambda_b^0 \to \Lambda_c^+ \pi^-$ and $\Lambda_b^0 \to D^0 p\pi^-$ branching fractions, the ratio of proton efficiencies is taken from simulation. For the calculation of the ratios $\mathcal{B}(\Lambda_b^0 \to D^0 pK^-)/\mathcal{B}(\Lambda_b^0 \to D^0 p\pi^-)$ and $\mathcal{B}(\Lambda_b^0 \to \Lambda_c^+ K^-)/\mathcal{B}(\Lambda_b^0 \to \Lambda_c^+ \pi^-)$, where the kinematic properties of the proton track for the decays in the numerator and denominator are similar, the efficiencies are taken to be equal.

The simulated samples used to obtain the selection efficiency are generated with phase-space models for the three-body $\Lambda_b^0 \to D^0 ph^-$ and $\Lambda_c^+ \to pK^-\pi^+$ decays. The

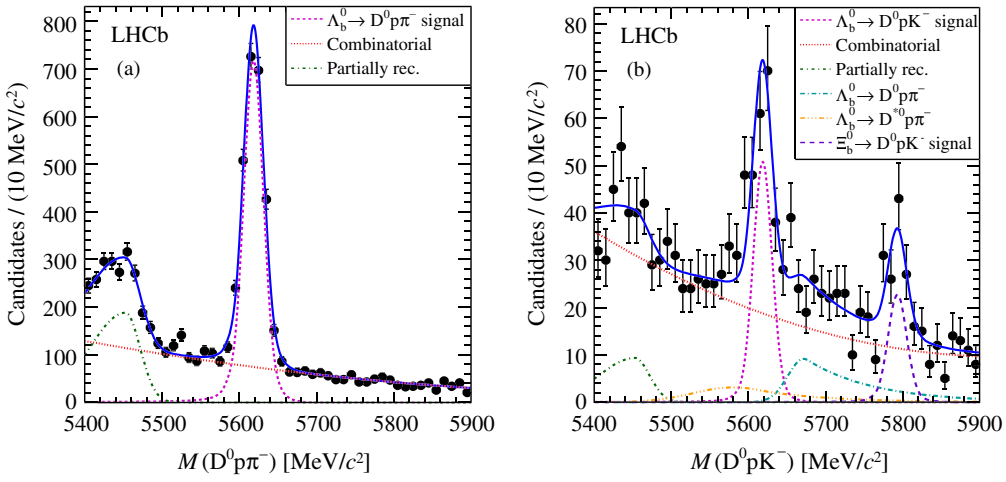

FIG. 2 (color online). Distributions of invariant mass for (a) $D^0 p\pi^-$ and (b) $D^0 pK^-$ candidates passing the tight selection (points with error bars) and results of the fit (solid line). The signal and background contributions are shown.

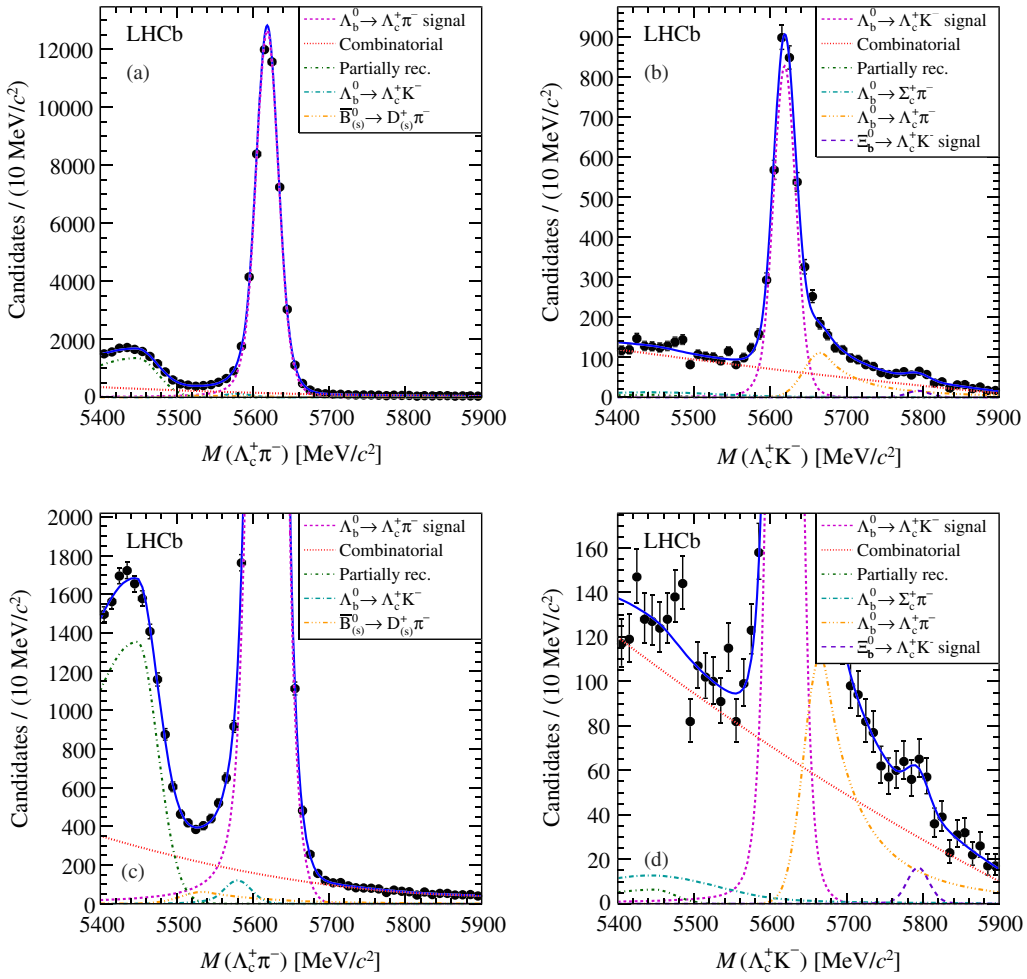

FIG. 3 (color online). Distributions of invariant mass for (a) $\Lambda_c^+\pi^-$ and (b) $\Lambda_c^+K^-$ candidates passing the tight selection (points with error bars) and results of the fit (solid line). The signal and background contributions are shown. The same distributions are magnified in (c) and (d) to better distinguish background components and $\Xi_b^0 \to \Lambda_c^+K^-$ signal.

three-body distributions in data are, however, significantly nonuniform. Therefore, the efficiency obtained from the simulation has to be corrected for the dependence on the three-body decay kinematic properties. In the case of $\Lambda_b^0 \to D^0p\pi^-$ decays, the relative selection efficiency as a function of D^0p and $p\pi^-$ squared invariant masses $\varepsilon[M^2(D^0p), M^2(p\pi^-)]$ is determined from the phase-space simulated sample and parametrized with a polynomial function of fourth order. The function $\varepsilon[M^2(D^0p), M^2(p\pi^-)]$ is normalized such that its integral is unity over the kinematically allowed phase space. The efficiency correction factor $\varepsilon_{\rm PS}$ is calculated as

$$\varepsilon_{\rm PS} = \frac{\sum_i w_i}{\sum_i w_i/\varepsilon[M_i^2(D^0p), M_i^2(p\pi^-)]}, \tag{7}$$

where $M_i^2(D^0p)$ and $M_i^2(p\pi^-)$ are the squared invariant masses of the D^0p and $p\pi^-$ combinations for the ith event in data and w_i is its signal weight obtained from the $M(D^0ph^-)$ invariant mass fit. The correction factor for the $\Lambda_c^+ \to pK^-\pi^+$ decay is calculated similarly.

Since the three-body decays $\Lambda_c^+ \to pK^-\pi^+$ and $\Lambda_b^0 \to D^0ph^-$ involve particles with nonzero spin in the initial and final states, the kinematic properties of these decays are

TABLE II. Results of the fit to the invariant mass distributions of $\Lambda_b^0 \to \Lambda_c^+h^-$ and $\Lambda_b^0 \to D^0ph^-$ candidates passing the tight selection. The uncertainties are statistical only.

Decay mode	Yield
$\Lambda_b^0 \to D^0p\pi^-$	2452 ± 58
$\Lambda_b^0 \to \Lambda_c^+\pi^-$	$50\,072 \pm 253$
$\Lambda_b^0 \to D^0pK^-$	163 ± 18
$\Lambda_b^0 \to \Lambda_c^+K^-$	3182 ± 66
$\Xi_b^0 \to D^0pK^-$	74 ± 13
$\Xi_b^0 \to \Lambda_c^+K^-$	62 ± 20
Particle	**Mass [MeV/c^2]**
Λ_b^0	5618.7 ± 0.1
Ξ_b^0	5793.5 ± 2.3

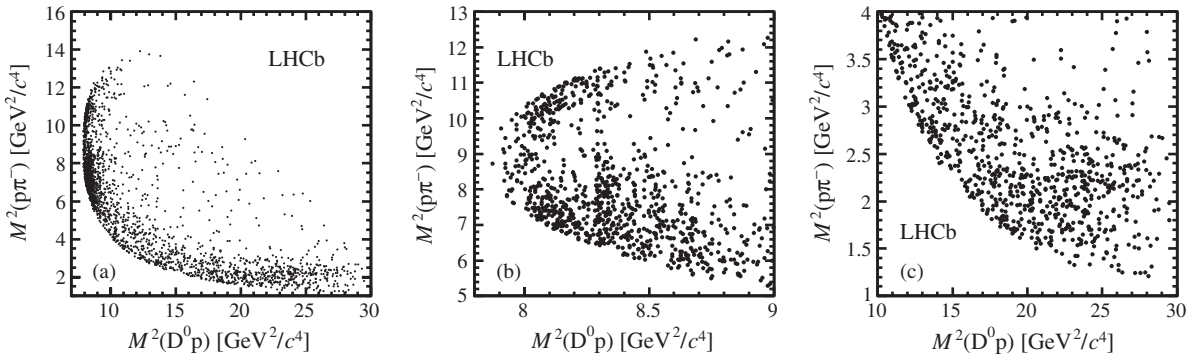

FIG. 4. Dalitz plot of $\Lambda_b^0 \to D^0 p\pi^-$ candidates in (a) the full phase space region and magnified regions of (b) low $M^2(D^0p)$ and (c) low $M^2(p\pi^-)$.

described by angular variables in addition to the two Dalitz plot variables. The variation of the selection efficiency with the angles can thus affect the measurement. We use three independent variables to parametrize the angular phase space, similar to those used in Ref. [31] for the analysis of the $\Lambda_c^+ \to pK^-\pi^+$ decay. The variables are defined in the rest frame of the decaying Λ_b^0 or Λ_c^+ baryons, with the x axis given by their direction in the laboratory frame, the polarization axis z given by the cross product of the beam and x axes, and the y axis given by the cross product of the z and x axes. The three variables are the cosine of the polar angle θ_p of the proton momentum in this reference frame, the azimuthal angle φ_p of the proton momentum in the reference frame, and the angle between the D^0h^- plane (for $\Lambda_b^0 \to D^0 ph^-$) or $K^-\pi^+$ plane (for $\Lambda_c^+ \to pK^-\pi^+$) and the plane formed by the proton and polarization axis.

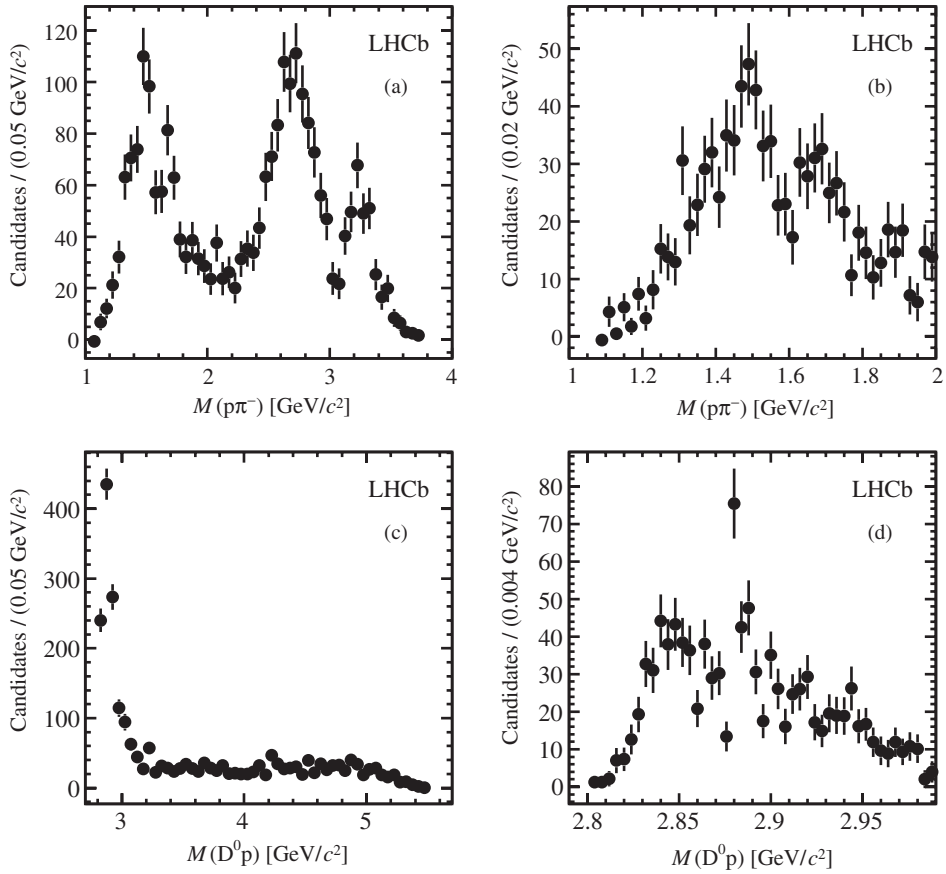

FIG. 5. Background-subtracted distributions of (a,b) $M(p\pi^-)$ and (c,d) $M(D^0p)$ invariant masses in $\Lambda_b^0 \to D^0 p\pi^-$ decays, where (b) and (d) are versions of (a) and (c), respectively, showing the lower invariant mass parts of the distributions. The distributions are not corrected for efficiency.

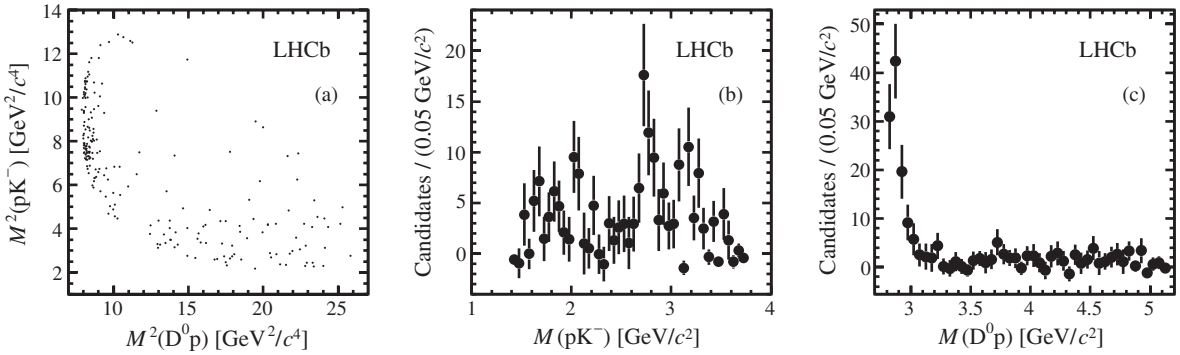

FIG. 6. (a) $\Lambda_b^0 \to D^0 p K^-$ Dalitz plot and background-subtracted distributions of (b) $M(pK^-)$ and (c) $M(D^0 p)$ invariant masses. The distributions are not corrected for efficiency.

The angular acceptance corrections are calculated from background-subtracted angular distributions obtained from the data. The distributions are similar to those obtained from the simulation of unpolarized Λ_b^0 decays, supporting the observation of small Λ_b^0 polarization in pp collisions [32]. The angular corrections are found to be negligible and are not used in the calculation of the ratios of branching fractions.

The values of the efficiency correction factors are given in Table III. The values of the branching fraction ratios defined in Eqs. (2–5), obtained after corrections as described above, and their statistical uncertainties are given in Table IV.

VI. SYSTEMATIC UNCERTAINTIES

The systematic uncertainties in the measurements of the ratios of branching fractions are listed in Table IV.

The uncertainties due to the description of signal and background contributions in the invariant mass fit model are estimated as follows:

(i) The uncertainty due to the parametrization of the signal distributions is obtained by using an alternative description based on a double-Gaussian shape, or a triple-Gaussian shape in the case of $\Lambda_b^0 \to \Lambda_c^+ \pi^-$.

(ii) To determine the uncertainty due to the combinatorial background parametrization, an alternative model with an exponential distribution is used instead of the quadratic polynomial function.

(iii) The uncertainty in the parametrization of the backgrounds from B meson decays with misidentified particles in the final state is estimated by removing the $\bar{B}^0_{(s)} \to D^+_{(s)} \pi^-$ contribution. The uncertainty due to the parametrizaton of the K/π misidentification background is estimated by using the shapes obtained without the PID requirements and without rejecting the events with the $D^0 p$ invariant mass squared greater than 10 GeV$^2/c^4$ in the fit to the simulated sample.

(iv) The uncertainty due to the partially reconstructed background is estimated by fitting the invariant mass distributions in the reduced range of 5500–5900 MeV/c^2 and by excluding the contributions of partially reconstructed backgrounds with K/π misidentification from the fit for $D^0 p K^-$ and $\Lambda_c^+ K^-$ combinations.

(v) The uncertainty due to the charmless background component $\Lambda_b^0 \to p K^- \pi^+ h^-$ is estimated from the fit of the $D^0 p h^-$ ($\Lambda_c^+ h^-$) invariant mass distributions in the sidebands of the D^0 (Λ_c^+) candidate invariant mass.

A potential source of background that is not included in the fit comes from Ξ_b^0 baryon decays into $D^{*0} p K^-$ or similar final states, which differ from the reconstructed $D^0 p K^-$ state by missing low-momentum particles. Such decays can contribute under the $\Lambda_b^0 \to D^0 p K^-$ signal peak. The possible contribution of these decays is estimated assuming that $\mathcal{B}(\Xi_b^0 \to D^{*0} p K^-)/\mathcal{B}(\Xi_b^0 \to D^0 p K^-)$ is equal to $\mathcal{B}(\Lambda_b^0 \to D^{*0} p K^-)/\mathcal{B}(\Lambda_b^0 \to D^0 p K^-)$ and that the selection efficiencies for Ξ_b^0 and Λ_b^0 decays are the same. The one-sided systematic uncertainty due to this effect is added to the background model uncertainty for the $\Lambda_b^0 \to D^0 p K^-$ decay mode.

TABLE III. Efficiency correction factors used to calculate the ratios of branching fractions.

Correction factor	$R_{\Lambda_b^0 \to D^0 p \pi^-}$	$R_{\Lambda_b^0 \to D^0 p K^-}$	$R_{\Lambda_b^0 \to \Lambda_c^+ K^-}$	$R_{\Xi_b^0 \to D^0 p K^-}$	$R_{\Xi_b^0 \to \Lambda_c^+ K^-}$
$\varepsilon^i_{\mathrm{sel}}/\varepsilon^j_{\mathrm{sel}}$	1.18	1.01	0.99	0.97	0.68
$\varepsilon^i_{\mathrm{PID}}/\varepsilon^j_{\mathrm{PID}}$	0.98	1.06	1.17	–	1.07
$\varepsilon^i_{\mathrm{PS}}/\varepsilon^j_{\mathrm{PS}}$	1.03	1.02	–	–	0.92

TABLE IV. Measured ratios of branching fractions, with their statistical and systematic uncertainties in units of 10^{-2}.

	$R_{\Lambda_b^0\to D^0 p\pi^-}$	$R_{\Lambda_b^0\to D^0 pK^-}$	$R_{\Lambda_b^0\to \Lambda_c^+ K^-}$	$R_{\Xi_b^0\to D^0 pK^-}$	$R_{\Xi_b^0\to \Lambda_c^+ K^-}$
Central value	8.06	7.27	7.31	44.3	57
Statistical uncertainty	0.23	0.82	0.16	9.2	22
Systematic uncertainties					
Signal model	0.03	0.03	0.05	0.2	3
Background model	0.07	$^{+0.34}_{-0.54}$	0.09	5.0	20
Trigger efficiency	0.01	0.08	0.07	<0.1	<1
Reconstruction efficiency	<0.01	0.04	0.04	<0.1	<1
Selection efficiency	0.12	0.01	<0.01	<0.1	<1
Simulation sample size	0.06	0.07	0.08	0.6	<1
Phase space acceptance	0.07	0.04	–	<0.1	<1
Angular acceptance	0.15	0.29	–	3.5	4
PID efficiency	0.26	0.11	0.04	–	1
Total systematic uncertainty	0.35	$^{+0.48}_{-0.64}$	0.16	6.0	21

The trigger efficiency uncertainty is dominated by the difference of the transverse energy threshold of the hardware-stage trigger observed between simulation and data. It is estimated by varying the transverse energy threshold in the simulation by 15%. In the case of measuring the ratios $R_{\Lambda_b^0\to D^0 pK^-}$ and $R_{\Lambda_b^0\to \Lambda_c^+ K^-}$, one also has to take into account the difference of hadronic interaction cross section for kaons and pions before the calorimeter. This difference is studied using a sample of $B^+\to \bar{D}^0\pi^+$, $\bar{D}^0\to K^+\pi^-$ decays that pass the trigger decision independent of the final-state particles of these decays. The difference was found to be 4.5% for $D^0 ph^-$ and 2.5% for $\Lambda_c^+ h^-$. Since only about 13% of events are triggered exclusively by the h^- particle, the resulting uncertainty is low.

The uncertainty due to track reconstruction efficiency cancels to a good approximation for the quoted ratios since the track multiplicities of the decays are the same. However, for the ratios $R_{\Lambda_b^0\to D^0 pK^-}$ and $R_{\Lambda_b^0\to \Lambda_c^+ K^-}$, the difference in the hadronic interaction rate for kaons and pions in the tracker can bias the measurement. A systematic uncertainty is assigned taking into account the rate of hadronic interactions in the simulation and the uncertainty on the knowledge of the amount of material in the LHCb tracker.

The uncertainty in the selection efficiency obtained from simulation is evaluated by scaling the variables that enter the offline selection. The scaling factor is chosen from the comparison of the distributions of these variables in simulation and in a background-subtracted $\Lambda_b^0\to\Lambda_c^+\pi^-$ sample. In addition, the uncertainty due to the finite size of the simulation samples is assigned.

The uncertainty of the phase-space efficiency correction includes four effects. The statistical uncertainty on the correction factor is determined by the data sample size and variations of the efficiency over the phase space. The uncertainty in the parametrization of the efficiency shape is estimated by using an alternative parametrization with a third-order rather than a fourth-order polynomial. The correlation of the efficiency shape and invariant mass of Λ_b^0 (Ξ_b^0) candidates is estimated by calculating the efficiency shape in three bins of Λ_b^0 (Ξ_b^0) mass separately and using one of the three shapes depending on the invariant mass of the candidate. The uncertainty due to the difference of the Λ_b^0 (Ξ_b^0) kinematic properties between simulation and data is estimated by using the efficiency shape obtained after weighting the simulated sample using the momentum distribution of Λ_b^0 (Ξ_b^0) from background-subtracted $\Lambda_b^0\to\Lambda_c^+\pi^-$ data.

Corrections due to the angular acceptance in the calculation of ratios of branching fractions are consistent with zero. The central values quoted do not include these corrections, while the systematic uncertainty is evaluated by taking the maximum of the statistical uncertainty for the correction, determined by the size of the data sample, and the deviation of its central value from unity.

The uncertainty in the PID response is calculated differently for the ratio of $\Lambda_b^0\to D^0 p\pi^-$ and $\Lambda_b^0\to\Lambda_c^+\pi^-$ branching fractions using loose selection and for the measurements using tight BDT-based selections. For the ratio of $\Lambda_b^0\to D^0 p\pi^-$ and $\Lambda_b^0\to\Lambda_c^+\pi^-$ branching fractions, $R_{\Lambda_b^0\to D^0 p\pi^-}$, the uncertainty due to the pion and kaon PID requirements is estimated by scaling the PID variables within the limits given by the comparison of distributions from the reweighted calibration sample and the background-subtracted $\Lambda_b^0\to\Lambda_c^+\pi^-$ data. The dominant contribution to the PID uncertainty comes from the uncertainty in the proton PID efficiency ratio, which is caused by the difference in kinematic properties of the proton from $\Lambda_b^0\to D^0 p\pi^-$ and $\Lambda_b^0\to\Lambda_c^+\pi^-$ decays. The proton efficiency ratio in this case is taken from simulation, and the systematic uncertainty is estimated by taking this ratio to be equal to 1. In the case of measuring the ratios $R_{\Lambda_b^0\to D^0 pK^-}$

TABLE V. Systematic uncertainties in the measurement of the mass difference $m_{\Xi_b^0} - m_{\Lambda_b^0}$.

Source	Uncertainty (MeV/c^2)
Signal model	0.19
Background model	0.50
Momentum scale calibration	0.03
Total	0.54

and $R_{\Lambda_b^0 \to \Lambda_c^+ K^-}$, the uncertainty due to the proton PID and the tracks coming from the D^0 or Λ_c^+ candidates is negligible due to similar kinematic distributions of the decays in the numerator and denominator. The dominant contribution comes from the PID efficiency ratio for the kaon or pion track from the Λ_b^0 vertex; this is estimated by scaling the PID distribution as described above. In addition, there are contributions due to the finite size of the PID calibration sample and the uncertainty due to assumption that the PID efficiency for the individual tracks factorizes in the total efficiency. The latter is estimated with simulated samples.

Since the results for the Λ_b^0 decay modes are all ratios to other Λ_b^0 decays, there is no systematic bias introduced by the dependence of the efficiency on the Λ_b^0 lifetime and the fact that the value used in the simulation (1.38 ps) differs from the latest measurement [33]. We also do not assign any systematic uncertainty due to the lack of knowledge of the Ξ_b^0 lifetime, which is as yet unmeasured (a value of 1.42 ps is used in the simulation).

The dominant systematic uncertainties in the measurement of the Ξ_b^0 and Λ_b^0 mass difference (see Table V) come from the uncertainties of the signal and background models and are estimated from the same variations of these models as in the calculation of branching fractions. The uncertainty due to the momentum scale calibration partially cancels in the quoted difference of Ξ_b^0 and Λ_b^0 masses; the residual contribution is estimated by varying the momentum scale factor within its uncertainty of 0.3% [24].

VII. SIGNAL SIGNIFICANCE AND FIT VALIDATION

The statistical significance of the $\Lambda_b^0 \to D^0 p K^-$, $\Xi_b^0 \to D^0 p K^-$, and $\Xi_b^0 \to \Lambda_c^+ K^-$ signals, expressed in terms of equivalent number of standard deviations (σ), is evaluated from the maximum likelihood fit as

$$S_{\text{stat}} = \sqrt{-2\Delta \ln \mathcal{L}}, \tag{8}$$

where $\Delta \ln \mathcal{L}$ is the difference in logarithms of the likelihoods for the fits with and without the corresponding signal contribution. The fit yields the statistical significance of the $\Lambda_b^0 \to D^0 p K^-$, $\Xi_b^0 \to D^0 p K^-$, and $\Xi_b^0 \to \Lambda_c^+ K^-$ signals of 10.8σ, 6.7σ, and 4.7σ, respectively.

The validity of this evaluation is checked with the following procedure. To evaluate the significance of each signal, a large number of invariant mass distributions is generated using the result of the fit on data as input, excluding the signal contribution under consideration. Each distribution is then fitted with models that include background only, as well as background and signal. The significance is obtained as the fraction of samples where the difference $\Delta \ln \mathcal{L}$ for the fits with and without the signal is larger than in data. The significance evaluated from the likelihood fit according to Eq. (8) is consistent with, or slightly smaller than, that estimated from the simulated experiments. Thus, the significance calculated as in Eq. (8) is taken.

The significance accounting for the systematic uncertainties is evaluated as

$$S_{\text{stat+syst}} = S_{\text{stat}} / \sqrt{1 + \sigma_{\text{syst}}^2 / \sigma_{\text{stat}}^2}, \tag{9}$$

where σ_{stat} is the statistical uncertainty of the signal yield and σ_{syst} is the corresponding systematic uncertainty, which only includes the relevant uncertainties due to the signal and background models. As a result, the significance for the $\Lambda_b^0 \to D^0 p K^-$, $\Xi_b^0 \to D^0 p K^-$, and $\Xi_b^0 \to \Lambda_c^+ K^-$ signals is calculated to be 9.0σ, 5.9σ, and 3.3σ, respectively.

The fitting procedure is tested with simulated experiments where the invariant mass distributions are generated from the PDFs that are a result of the data fit and then fitted with the same procedure as applied to data. No significant biases are introduced by the fit procedure in the fitted parameters. However, we find that the statistical uncertainty on the Ξ_b^0 mass is underestimated by 3% in the fit, and the uncertainty on the $\Xi_b^0 \to D^0 p K^-$ yield is underestimated by 5%. We apply the corresponding scale factors to the $\Xi_b^0 \to D^0 p K^-$ yield and Ξ_b^0 mass uncertainties to obtain the final results.

VIII. CONCLUSION

We report studies of beauty baryon decays to the $D^0 p h^-$ and $\Lambda_c^+ h^-$ final states, using a data sample corresponding to an integrated luminosity of 1.0 fb^{-1} collected with the LHCb detector. First observations of the $\Lambda_b^0 \to D^0 p K^-$ and $\Xi_b^0 \to D^0 p K^-$ decays are reported, with significances of 9.0 and 5.9 standard deviations, respectively. The decay $\Lambda_b^0 \to \Lambda_c^+ K^-$ is observed for the first time; the significance of this observation is greater than 10 standard deviations. The first evidence for the $\Xi_b^0 \to \Lambda_c^+ K^-$ decay is also obtained with a significance of 3.3 standard deviations.

The combinations of branching and fragmentation fractions for beauty baryons decaying into $D^0 p h^-$ and $\Lambda_c^+ h^-$ final states are measured to be

$$R_{\Lambda_b^0\to D^0 p\pi^-} \equiv \frac{\mathcal{B}(\Lambda_b^0 \to D^0 p\pi^-) \times \mathcal{B}(D^0 \to K^-\pi^+)}{\mathcal{B}(\Lambda_b^0 \to \Lambda_c^+\pi^-) \times \mathcal{B}(\Lambda_c^+ \to pK^-\pi^+)} = 0.0806 \pm 0.0023 \pm 0.0035,$$

$$R_{\Lambda_b^0\to D^0 pK^-} \equiv \frac{\mathcal{B}(\Lambda_b^0 \to D^0 pK^-)}{\mathcal{B}(\Lambda_b^0 \to D^0 p\pi^-)} = 0.073 \pm 0.008^{+0.005}_{-0.006},$$

$$R_{\Lambda_b^0\to \Lambda_c^+ K^-} \equiv \frac{\mathcal{B}(\Lambda_b^0 \to \Lambda_c^+ K^-)}{\mathcal{B}(\Lambda_b^0 \to \Lambda_c^+ \pi^-)} = 0.0731 \pm 0.0016 \pm 0.0016,$$

$$R_{\Xi_b^0\to D^0 pK^-} \equiv \frac{f_{\Xi_b^0} \times \mathcal{B}(\Xi_b^0 \to D^0 pK^-)}{f_{\Lambda_b^0} \times \mathcal{B}(\Lambda_b^0 \to D^0 pK^-)} = 0.44 \pm 0.09 \pm 0.06,$$

$$R_{\Xi_b^0\to \Lambda_c^+ K^-} \equiv \frac{\mathcal{B}(\Xi_b^0 \to \Lambda_c^+ K^-) \times \mathcal{B}(\Lambda_c^+ \to pK^-\pi^+)}{\mathcal{B}(\Xi_b^0 \to D^0 pK^-) \times \mathcal{B}(D^0 \to K^-\pi^+)} = 0.57 \pm 0.22 \pm 0.21,$$

where the first uncertainty is statistical and the second systematic. The ratios of the Cabibbo-suppressed to Cabibbo-favored branching fractions for both the $D^0 ph^-$ and the $\Lambda_c^+ h^-$ modes are consistent with the those observed for the $B \to Dh$ modes [1]. In addition, the difference of Ξ_b^0 and Λ_b^0 baryon masses is measured to be

$$m_{\Xi_b^0} - m_{\Lambda_b^0} = 174.8 \pm 2.4 \pm 0.5 \text{ MeV}/c^2.$$

Using the latest LHCb measurement of the Λ_b^0 mass $m_{\Lambda_b^0} = 5619.53 \pm 0.13 \pm 0.45$ MeV$/c^2$ [24], the Ξ_b^0 mass is determined to be $m_{\Xi_b^0} = 5794.3 \pm 2.4 \pm 0.7$ MeV$/c^2$, in agreement with the measurement performed by CDF [3] and twice as precise.

ACKNOWLEDGMENTS

We express our gratitude to our colleagues in the CERN accelerator departments for the excellent performance of the LHC. We thank the technical and administrative staff at the LHCb institutes. We acknowledge support from CERN and from the national agencies: CAPES, CNPq, FAPERJ, and FINEP (Brazil); NSFC (China); CNRS/IN2P3 and Region Auvergne (France); BMBF, DFG, HGF, and MPG (Germany); SFI (Ireland); INFN (Italy); FOM and NWO (Netherlands); SCSR (Poland); MEN/IFA (Romania); MinES, Rosatom, RFBR, and NRC "Kurchatov Institute" (Russia); MinECo, XuntaGal, and GENCAT (Spain); SNSF and SER (Switzerland); NAS Ukraine (Ukraine); STFC (United Kingdom); NSF (USA). We also acknowledge the support received from the ERC under FP7. The Tier1 computing centers are supported by IN2P3 (France), KIT and BMBF (Germany), INFN (Italy), NWO and SURF (Netherlands), PIC (Spain), and GridPP (United Kingdom). We are thankful for the computing resources put at our disposal by Yandex LLC (Russia) as well as to the communities behind the multiple open-source software packages that we depend on.

[1] J. Beringer *et al.* (Particle Data Group), Phys. Rev. D **86**, 010001 (2012) and 2013 partial update for the 2014 edition.
[2] T. Aaltonen *et al.* (CDF Collaboration), Phys. Rev. Lett. **99**, 202001 (2007).
[3] T. Aaltonen *et al.* (CDF Collaboration), Phys. Rev. Lett. **107**, 102001 (2011).
[4] I. Dunietz, Z. Phys. C **56**, 129 (1992).
[5] Fayyazuddin, Mod. Phys. Lett. A **14**, 63 (1999).
[6] A. K. Giri, R. Mohanta, and M. P. Khanna, Phys. Rev. D **65**, 073029 (2002).
[7] I. Dunietz, Phys. Lett. B **270**, 75 (1991).
[8] T. Gershon, Phys. Rev. D **79**, 051301 (2009).
[9] T. Gershon and M. Williams, Phys. Rev. D **80**, 092002 (2009).
[10] A. A. Alves, Jr. *et al.* (LHCb Collaboration), JINST **3**, S08005 (2008).
[11] R. Aaij *et al.* (LHCb Collaboration), Phys. Rev. Lett. **109**, 172003 (2012).
[12] LHCb collaboration, Report No. LHCb-CONF-2012-029.
[13] M. Adinolfi *et al.*, Eur. Phys. J. C **73**, 2431 (2013).
[14] A. A. Alves, Jr., *et al.*, JINST **8**, P02022 (2013).
[15] R. Aaij *et al.*, JINST **8**, P04022 (2013).
[16] V. V. Gligorov and M. Williams, JINST **8**, P02013 (2013).
[17] T. Sjöstrand, S. Mrenna, and P. Skands, J. High Energy Phys. 05 (**2006**) 026.
[18] I. Belyaev *et al.*, *Nuclear Science Symposium Conference Record (NSS/MIC) (IEEE, New York, 2010) p. 1155.*
[19] D. J. Lange, Nucl. Instrum. Methods Phys. Res., Sect. A **462**, 152 (2001).
[20] J. Allison *et al.* (GEANT4 Collaboration), IEEE Trans. Nucl. Sci. **53**, 270 (2006).
[21] S. Agostinelli *et al.* (GEANT4 Collaboration), Nucl. Instrum. Methods Phys. Res., Sect. A **506**, 250 (2003).
[22] M. Clemencic, G. Corti, S. Easo, C. R. Jones, S. Miglioranzi, M. Pappagallo, and P. Robbe, J. Phys. Conf. Ser. **331**, 032023 (2011).
[23] W. D. Hulsbergen, Nucl. Instrum. Methods Phys. Res., Sect. A **552**, 566 (2005).
[24] R. Aaij *et al.* (LHCb Collaboration), Phys. Rev. Lett. **110**, 182001 (2013).
[25] L. Breiman, J. H. Friedman, R. A. Olshen, and C. J. Stone, *Classification and Regression Trees* (, Belmont, CA, 1984).

[26] T. Skwarnicki, Ph.D. thesis, Institute of Nuclear Physics, Krakow, Poland, 1986, DESY-F31-86-02.
[27] R. Aaij *et al.* (LHCb Collaboration), Phys. Rev. Lett. **109**, 131801 (2012).
[28] R. Aaij *et al.* (LHCb Collaboration), Phys. Rev. D **87**, 112009 (2013).
[29] R. Aaij *et al.* (LHCb Collaboration), J. High Energy Phys. 04 (**2013**) 1.
[30] M. Pivk and F. R. Le Diberder, Nucl. Instrum. Methods Phys. Res., Sect. A **555**, 356 (2005).
[31] E. Aitala *et al.* (E791 Collaboration), Phys. Lett. B **471**, 449 (2000).
[32] R. Aaij *et al.* (LHCb Collaboration), Phys. Lett. B **724**, 27 (2013).
[33] R. Aaij *et al.* (LHCb Collaboration), Phys. Rev. Lett. **111**, 102003 (2013).

R. Aaij,[40] B. Adeva,[36] M. Adinolfi,[45] C. Adrover,[6] A. Affolder,[51] Z. Ajaltouni,[5] J. Albrecht,[9] F. Alessio,[37] M. Alexander,[50] S. Ali,[40] G. Alkhazov,[29] P. Alvarez Cartelle,[36] A. A. Alves Jr.,[24] S. Amato,[2] S. Amerio,[21] Y. Amhis,[7] L. Anderlini,[17,f] J. Anderson,[39] R. Andreassen,[56] M. Andreotti,[16,e] J. E. Andrews,[57] R. B. Appleby,[53] O. Aquines Gutierrez,[10] F. Archilli,[37] A. Artamonov,[34] M. Artuso,[58] E. Aslanides,[6] G. Auriemma,[24,m] M. Baalouch,[5] S. Bachmann,[11] J. J. Back,[47] A. Badalov,[35] V. Balagura,[30] W. Baldini,[16] R. J. Barlow,[53] C. Barschel,[38] S. Barsuk,[7] W. Barter,[46] V. Batozskaya,[27] T. Bauer,[40] A. Bay,[38] J. Beddow,[50] F. Bedeschi,[22] I. Bediaga,[1] S. Belogurov,[30] K. Belous,[34] I. Belyaev,[30] E. Ben-Haim,[8] G. Bencivenni,[18] S. Benson,[49] J. Benton,[45] A. Berezhnoy,[31] R. Bernet,[39] M.-O. Bettler,[46] M. van Beuzekom,[40] A. Bien,[11] S. Bifani,[44] T. Bird,[53] A. Bizzeti,[17,h] P. M. Bjørnstad,[53] T. Blake,[47] F. Blanc,[38] J. Blouw,[10] S. Blusk,[58] V. Bocci,[24] A. Bondar,[33] N. Bondar,[29] W. Bonivento,[15,37] S. Borghi,[53] A. Borgia,[58] T. J. V. Bowcock,[51] E. Bowen,[39] C. Bozzi,[16] T. Brambach,[9] J. van den Brand,[41] J. Bressieux,[38] D. Brett,[53] M. Britsch,[10] T. Britton,[58] N. H. Brook,[45] H. Brown,[51] A. Bursche,[39] G. Busetto,[21,q] J. Buytaert,[37] S. Cadeddu,[15] R. Calabrese,[16,e] O. Callot,[7] M. Calvi,[20,j] M. Calvo Gomez,[35,o] A. Camboni,[35] P. Campana,[18,37] D. Campora Perez,[37] A. Carbone,[14,c] G. Carboni,[23,k] R. Cardinale,[19,i] A. Cardini,[15] H. Carranza-Mejia,[49] L. Carson,[52] K. Carvalho Akiba,[2] G. Casse,[51] L. Castillo Garcia,[37] M. Cattaneo,[37] C. Cauet,[9] R. Cenci,[57] M. Charles,[8] P. Charpentier,[37] S.-F. Cheung,[54] N. Chiapolini,[39] M. Chrzaszcz,[39,25] K. Ciba,[37] X. Cid Vidal,[37] G. Ciezarek,[52] P. E. L.Clarke,[49] M. Clemencic,[37] H. V. Cliff,[46] J. Closier,[37] C. Coca,[28] V. Coco,[40] J. Cogan,[6] E. Cogneras,[5] P. Collins,[37] A. Comerma-Montells,[35] A. Contu,[15,37] A. Cook,[45] M. Coombes,[45] S. Coquereau,[8] G. Corti,[37] B. Couturier,[37] G. A. Cowan,[49] D. C. Craik,[47] M. Cruz Torres,[59] S. Cunliffe,[52] R. Currie,[49] C. D'Ambrosio,[37] J. Dalseno,[45] P. David,[8] P. N. Y. David,[40] A. Davis,[56] I. De Bonis,[4] K. De Bruyn,[40] S. De Capua,[53] M. De Cian,[11] J. M. De Miranda,[1] L. De Paula,[2] W. De Silva,[56] P. De Simone,[18] D. Decamp,[4] M. Deckenhoff,[9] L. Del Buono,[8] N. Déléage,[4] D. Derkach,[54] O. Deschamps,[5] F. Dettori,[41] A. Di Canto,[11] H. Dijkstra,[37] M. Dogaru,[28] S. Donleavy,[51] F. Dordei,[11] P. Dorosz,[25,n] A. Dosil Suárez,[36] D. Dossett,[47] A. Dovbnya,[42] F. Dupertuis,[38] P. Durante,[37] R. Dzhelyadin,[34] A. Dziurda,[25] A. Dzyuba,[29] S. Easo,[48] U. Egede,[52] V. Egorychev,[30] S. Eidelman,[33] D. van Eijk,[40] S. Eisenhardt,[49] U. Eitschberger,[9] R. Ekelhof,[9] L. Eklund,[50,37] I. El Rifai,[5] C. Elsasser,[39] A. Falabella,[14,e] C. Färber,[11] C. Farinelli,[40] S. Farry,[51] D. Ferguson,[49] V. Fernandez Albor,[36] F. Ferreira Rodrigues,[1] M. Ferro-Luzzi,[37] S. Filippov,[32] M. Fiore,[16,e] M. Fiorini,[16,e] C. Fitzpatrick,[37] M. Fontana,[10] F. Fontanelli,[19,i] R. Forty,[37] O. Francisco,[2] M. Frank,[37] C. Frei,[37] M. Frosini,[17,37,f] E. Furfaro,[23,k] A. Gallas Torreira,[36] D. Galli,[14,c] M. Gandelman,[2] P. Gandini,[58] Y. Gao,[3] J. Garofoli,[58] P. Garosi,[53] J. Garra Tico,[46] L. Garrido,[35] C. Gaspar,[37] R. Gauld,[54] E. Gersabeck,[11] M. Gersabeck,[53] T. Gershon,[47] P. Ghez,[4] V. Gibson,[46] L. Giubega,[28] V. V. Gligorov,[37] C. Göbel,[59] D. Golubkov,[30] A. Golutvin,[52,30,37] A. Gomes,[2] H. Gordon,[37] M. Grabalosa Gándara,[5] R. Graciani Diaz,[35] L. A. Granado Cardoso,[37] E. Graugés,[35] G. Graziani,[17] A. Grecu,[28] E. Greening,[54] S. Gregson,[46] P. Griffith,[44] L. Grillo,[11] O. Grünberg,[60] B. Gui,[58] E. Gushchin,[32] Y. Guz,[34,37] T. Gys,[37] C. Hadjivasiliou,[58] G. Haefeli,[38] C. Haen,[37] T. W. Hafkenscheid,[62] S. C. Haines,[46] S. Hall,[52] B. Hamilton,[57] T. Hampson,[45] S. Hansmann-Menzemer,[11] N. Harnew,[54] S. T. Harnew,[45] J. Harrison,[53] T. Hartmann,[60] J. He,[37] T. Head,[37] V. Heijne,[40] K. Hennessy,[51] P. Henrard,[5] J. A.Hernando Morata,[36] E. van Herwijnen,[37] M. Heß,[60] A. Hicheur,[1] E. Hicks,[51] D. Hill,[54] M. Hoballah,[5] C. Hombach,[53] W. Hulsbergen,[40] P. Hunt,[54] T. Huse,[51] N. Hussain,[54] D. Hutchcroft,[51] D. Hynds,[50] V. Iakovenko,[43] M. Idzik,[26] P. Ilten,[55] R. Jacobsson,[37] A. Jaeger,[11] E. Jans,[40] P. Jaton,[38] A. Jawahery,[57] F. Jing,[3] M. John,[54] D. Johnson,[54] C. R. Jones,[46] C. Joram,[37] B. Jost,[37] N. Jurik,[58] M. Kaballo,[9] S. Kandybei,[42] W. Kanso,[6] M. Karacson,[37] T. M. Karbach,[37] I. R. Kenyon,[44] T. Ketel,[41] B. Khanji,[20] S. Klaver,[53] O. Kochebina,[7] I. Komarov,[38] R. F. Koopman,[41] P. Koppenburg,[40] M. Korolev,[31] A. Kozlinskiy,[40] L. Kravchuk,[32] K. Kreplin,[11] M. Kreps,[47] G. Krocker,[11] P. Krokovny,[33] F. Kruse,[9] M. Kucharczyk,[20,25,37,j] V. Kudryavtsev,[33] K. Kurek,[27] T. Kvaratskheliya,[30,37] V. N. La Thi,[38] D. Lacarrere,[37] G. Lafferty,[53] A. Lai,[15] D. Lambert,[49] R. W. Lambert,[41] E. Lanciotti,[37] G. Lanfranchi,[18] C. Langenbruch,[37] T. Latham,[47] C. Lazzeroni,[44] R. Le Gac,[6] J. van Leerdam,[40] J.-P. Lees,[4] R. Lefèvre,[5] A. Leflat,[31] J. Lefrançois,[7] S. Leo,[22] O. Leroy,[6] T. Lesiak,[25] B. Leverington,[11] Y. Li,[3] L. Li Gioi,[5] M. Liles,[51] R. Lindner,[37] C. Linn,[11] F. Lionetto,[39] B. Liu,[3] G. Liu,[37] S. Lohn,[37] I. Longstaff,[50] J. H. Lopes,[2] N. Lopez-March,[38] H. Lu,[3] D. Lucchesi,[21,q] J. Luisier,[38] H. Luo,[49] E. Luppi,[16,e] O. Lupton,[54] F. Machefert,[7] I. V. Machikhiliyan,[30] F. Maciuc,[28] O. Maev,[29,37] S. Malde,[54] G. Manca,[15,d] G. Mancinelli,[6] J. Maratas,[5]

U. Marconi,[14] P. Marino,[22,s] R. Märki,[38] J. Marks,[11] G. Martellotti,[24] A. Martens,[8] A. Martín Sánchez,[7] M. Martinelli,[40] D. Martinez Santos,[41,37] D. Martins Tostes,[2] A. Martynov,[31] A. Massafferri,[1] R. Matev,[37] Z. Mathe,[37] C. Matteuzzi,[20] E. Maurice,[6] A. Mazurov,[16,37,e] M. McCann,[52] J. McCarthy,[44] A. McNab,[53] R. McNulty,[12] B. McSkelly,[51] B. Meadows,[56,54] F. Meier,[9] M. Meissner,[11] M. Merk,[40] D. A. Milanes,[8] M.-N. Minard,[4] J. Molina Rodriguez,[59] S. Monteil,[5] D. Moran,[53] P. Morawski,[25] A. Mordà,[6] M. J. Morello,[22,s] R. Mountain,[58] I. Mous,[40] F. Muheim,[49] K. Müller,[39] R. Muresan,[28] B. Muryn,[26] B. Muster,[38] P. Naik,[45] T. Nakada,[38] R. Nandakumar,[48] I. Nasteva,[1] M. Needham,[49] S. Neubert,[37] N. Neufeld,[37] A. D. Nguyen,[38] T. D. Nguyen,[38] C. Nguyen-Mau,[38,p] M. Nicol,[7] V. Niess,[5] R. Niet,[9] N. Nikitin,[31] T. Nikodem,[11] A. Nomerotski,[54] A. Novoselov,[34] A. Oblakowska-Mucha,[26] V. Obraztsov,[34] S. Oggero,[40] S. Ogilvy,[50] O. Okhrimenko,[43] R. Oldeman,[15,d] G. Onderwater,[62] M. Orlandea,[28] J. M. Otalora Goicochea,[2] P. Owen,[52] A. Oyanguren,[35] B. K. Pal,[58] A. Palano,[13,b] M. Palutan,[18] J. Panman,[37] A. Papanestis,[48,37] M. Pappagallo,[50] L.Pappalardo,[16] C. Parkes,[53] C. J. Parkinson,[52] G. Passaleva,[17] G. D. Patel,[51] M. Patel,[52] C. Patrignani,[19,i] C. Pavel-Nicorescu,[28] A. Pazos Alvarez,[36] A. Pearce,[53] A. Pellegrino,[40] G. Penso,[24,l] M. Pepe Altarelli,[37] S. Perazzini,[14,c] E. Perez Trigo,[36] A. Pérez-Calero Yzquierdo,[35] P. Perret,[5] M. Perrin-Terrin,[6] L. Pescatore,[44] E. Pesen,[63] G. Pessina,[20] K. Petridis,[52] A. Petrolini,[19,i] E. Picatoste Olloqui,[35] B. Pietrzyk,[4] T. Pilař,[47] D. Pinci,[24] S. Playfer,[49] M. Plo Casasus,[36] F. Polci,[8] G. Polok,[25] A. Poluektov,[47,33] E. Polycarpo,[2] A. Popov,[34] D. Popov,[10] B. Popovici,[28] C. Potterat,[35] A. Powell,[54] J. Prisciandaro,[38] A. Pritchard,[51] C. Prouve,[7] V. Pugatch,[43] A. Puig Navarro,[38] G. Punzi,[22,r] W. Qian,[4] B. Rachwal,[25] J. H. Rademacker,[45] B. Rakotomiaramanana,[38] M. S. Rangel,[2] I. Raniuk,[42] N. Rauschmayr,[37] G. Raven,[41] S. Redford,[54] S. Reichert,[53] M. M. Reid,[47] A. C. dos Reis,[1] S. Ricciardi,[48] A. Richards,[52] K. Rinnert,[51] V. Rives Molina,[35] D. A. Roa Romero,[5] P. Robbe,[7] D. A. Roberts,[57] A. B. Rodrigues,[1] E. Rodrigues,[53] P. Rodriguez Perez,[36] S. Roiser,[37] V. Romanovsky,[34] A.Romero Vidal,[36] M. Rotondo,[21] J. Rouvinet,[38] T. Ruf,[37] F. Ruffini,[22] H. Ruiz,[35] P. Ruiz Valls,[35] G. Sabatino,[24,k] J. J. Saborido Silva,[36] N. Sagidova,[29] P. Sail,[50] B. Saitta,[15,d] V. Salustino Guimaraes,[2] B. Sanmartin Sedes,[36] R. Santacesaria,[24] C. Santamarina Rios,[36] E. Santovetti,[23,k] M. Sapunov,[6] A. Sarti,[18] C. Satriano,[24,m] A. Satta,[23] M. Savrie,[16,e] D. Savrina,[30,31] M. Schiller,[41] H. Schindler,[37] M. Schlupp,[9] M. Schmelling,[10] B. Schmidt,[37] O. Schneider,[38] A. Schopper,[37] M.-H. Schune,[7] R. Schwemmer,[37] B. Sciascia,[18] A. Sciubba,[24] M. Seco,[36] A. Semennikov,[30] K. Senderowska,[26] I. Sepp,[52] N. Serra,[39] J. Serrano,[6] P. Seyfert,[11] M. Shapkin,[34] I. Shapoval,[16,42,e] Y. Shcheglov,[29] T. Shears,[51] L. Shekhtman,[33] O. Shevchenko,[42] V. Shevchenko,[61] A. Shires,[9] R. Silva Coutinho,[47] M. Sirendi,[46] N. Skidmore,[45] T. Skwarnicki,[58] N. A. Smith,[51] E. Smith,[54,48] E. Smith,[52] J. Smith,[46] M. Smith,[53] M. D. Sokoloff,[56] F. J. P.Soler,[50] F. Soomro,[38] D. Souza,[45] B. Souza De Paula,[2] B. Spaan,[9] A. Sparkes,[49] P. Spradlin,[50] F. Stagni,[37] S. Stahl,[11] O. Steinkamp,[39] S. Stevenson,[54] S. Stoica,[28] S. Stone,[58] B. Storaci,[39] S. Stracka,[22,37] M. Straticiuc,[28] U. Straumann,[39] V. K. Subbiah,[37] L. Sun,[56] W. Sutcliffe,[52] S. Swientek,[9] V. Syropoulos,[41] M. Szczekowski,[27] P. Szczypka,[38,37] D. Szilard,[2] T. Szumlak,[26] S. T'Jampens,[4] M. Teklishyn,[7] G. Tellarini,[16,e] E. Teodorescu,[28] F. Teubert,[37] C. Thomas,[54] E. Thomas,[37] J. van Tilburg,[11] V. Tisserand,[4] M. Tobin,[38] S. Tolk,[41] L. Tomassetti,[16,e] D. Tonelli,[37] S. Topp-Joergensen,[54] N. Torr,[54] E. Tournefier,[4,52] S. Tourneur,[38] M. T. Tran,[38] M. Tresch,[39] A. Tsaregorodtsev,[6] P. Tsopelas,[40] N. Tuning,[40,37] M. Ubeda Garcia,[37] A. Ukleja,[27] A. Ustyuzhanin,[61] U. Uwer,[11] V. Vagnoni,[14] G. Valenti,[14] A. Vallier,[7] R. Vazquez Gomez,[18] P. Vazquez Regueiro,[36] C. Vázquez Sierra,[36] S. Vecchi,[16] J. J. Velthuis,[45] M. Veltri,[17,g] G. Veneziano,[38] M. Vesterinen,[37] B. Viaud,[7] D. Vieira,[2] X. Vilasis-Cardona,[35,o] A. Vollhardt,[39] D. Volyanskyy,[10] D. Voong,[45] A. Vorobyev,[29] V. Vorobyev,[33] C. Voß,[60] H. Voss,[10] J. A. de Vries,[40] R. Waldi,[60] C. Wallace,[47] R. Wallace,[12] S. Wandernoth,[11] J. Wang,[58] D. R. Ward,[46] N. K. Watson,[44] A. D. Webber,[53] D. Websdale,[52] M. Whitehead,[47] J. Wicht,[37] J. Wiechczynski,[25] D. Wiedner,[11] L. Wiggers,[40] G. Wilkinson,[54] M. P. Williams,[47,48] M. Williams,[55] F. F. Wilson,[48] J. Wimberley,[57] J. Wishahi,[9] W. Wislicki,[27] M. Witek,[25] G. Wormser,[7] S. A. Wotton,[46] S. Wright,[46] S. Wu,[3] K. Wyllie,[37] Y. Xie,[49,37] Z. Xing,[58] Z. Yang,[3] X. Yuan,[3] O. Yushchenko,[34] M. Zangoli,[14] M. Zavertyaev,[10,a] F. Zhang,[3] L. Zhang,[58] W. C. Zhang,[12] Y. Zhang,[3] A. Zhelezov,[11] A. Zhokhov,[30] L. Zhong,[3] and A. Zvyagin[37] *

(LHCb Collaboration)

[1]*Centro Brasileiro de Pesquisas Físicas (CBPF), Rio de Janeiro, Brazil*
[2]*Universidade Federal do Rio de Janeiro (UFRJ), Rio de Janeiro, Brazil*
[3]*Center for High Energy Physics, Tsinghua University, Beijing, China*
[4]*LAPP, Université de Savoie, CNRS/IN2P3, Annecy-Le-Vieux, France*
[5]*Clermont Université, Université Blaise Pascal, CNRS/IN2P3, LPC, Clermont-Ferrand, France*
[6]*CPPM, Aix-Marseille Université, CNRS/IN2P3, Marseille, France*
[7]*LAL, Université Paris-Sud, CNRS/IN2P3, Orsay, France*
[8]*LPNHE, Université Pierre et Marie Curie, Université Paris Diderot, CNRS/IN2P3, Paris, France*
[9]*Fakultät Physik, Technische Universität Dortmund, Dortmund, Germany*
[10]*Max-Planck-Institut für Kernphysik (MPIK), Heidelberg, Germany*
[11]*Physikalisches Institut, Ruprecht-Karls-Universität Heidelberg, Heidelberg, Germany*

[12]*School of Physics, University College Dublin, Dublin, Ireland*
[13]*Sezione INFN di Bari, Bari, Italy*
[14]*Sezione INFN di Bologna, Bologna, Italy*
[15]*Sezione INFN di Cagliari, Cagliari, Italy*
[16]*Sezione INFN di Ferrara, Ferrara, Italy*
[17]*Sezione INFN di Firenze, Firenze, Italy*
[18]*Laboratori Nazionali dell'INFN di Frascati, Frascati, Italy*
[19]*Sezione INFN di Genova, Genova, Italy*
[20]*Sezione INFN di Milano Bicocca, Milano, Italy*
[21]*Sezione INFN di Padova, Padova, Italy*
[22]*Sezione INFN di Pisa, Pisa, Italy*
[23]*Sezione INFN di Roma Tor Vergata, Roma, Italy*
[24]*Sezione INFN di Roma La Sapienza, Roma, Italy*
[25]*Henryk Niewodniczanski Institute of Nuclear Physics Polish Academy of Sciences, Kraków, Poland*
[26]*AGH - University of Science and Technology, Faculty of Physics and Applied Computer Science, Kraków, Poland*
[27]*National Center for Nuclear Research (NCBJ), Warsaw, Poland*
[28]*Horia Hulubei National Institute of Physics and Nuclear Engineering, Bucharest-Magurele, Romania*
[29]*Petersburg Nuclear Physics Institute (PNPI), Gatchina, Russia*
[30]*Institute of Theoretical and Experimental Physics (ITEP), Moscow, Russia*
[31]*Institute of Nuclear Physics, Moscow State University (SINP MSU), Moscow, Russia*
[32]*Institute for Nuclear Research of the Russian Academy of Sciences (INR RAN), Moscow, Russia*
[33]*Budker Institute of Nuclear Physics (SB RAS) and Novosibirsk State University, Novosibirsk, Russia*
[34]*Institute for High Energy Physics (IHEP), Protvino, Russia*
[35]*Universitat de Barcelona, Barcelona, Spain*
[36]*Universidad de Santiago de Compostela, Santiago de Compostela, Spain*
[37]*European Organization for Nuclear Research (CERN), Geneva, Switzerland*
[38]*Ecole Polytechnique Fédérale de Lausanne (EPFL), Lausanne, Switzerland*
[39]*Physik-Institut, Universität Zürich, Zürich, Switzerland*
[40]*Nikhef National Institute for Subatomic Physics, Amsterdam, Netherlands*
[41]*Nikhef National Institute for Subatomic Physics and VU University Amsterdam, Amsterdam, Netherlands*
[42]*NSC Kharkiv Institute of Physics and Technology (NSC KIPT), Kharkiv, Ukraine*
[43]*Institute for Nuclear Research of the National Academy of Sciences (KINR), Kyiv, Ukraine*
[44]*University of Birmingham, Birmingham, United Kingdom*
[45]*H.H. Wills Physics Laboratory, University of Bristol, Bristol, United Kingdom*
[46]*Cavendish Laboratory, University of Cambridge, Cambridge, United Kingdom*
[47]*Department of Physics, University of Warwick, Coventry, United Kingdom*
[48]*STFC Rutherford Appleton Laboratory, Didcot, United Kingdom*
[49]*School of Physics and Astronomy, University of Edinburgh, Edinburgh, United Kingdom*
[50]*School of Physics and Astronomy, University of Glasgow, Glasgow, United Kingdom*
[51]*Oliver Lodge Laboratory, University of Liverpool, Liverpool, United Kingdom*
[52]*Imperial College London, London, United Kingdom*
[53]*School of Physics and Astronomy, University of Manchester, Manchester, United Kingdom*
[54]*Department of Physics, University of Oxford, Oxford, United Kingdom*
[55]*Massachusetts Institute of Technology, Cambridge, Massachusetts, United States*
[56]*University of Cincinnati, Cincinnati, Ohio, United States*
[57]*University of Maryland, College Park, Maryland, United States*
[58]*Syracuse University, Syracuse, New York, United States*
[59]*Pontifícia Universidade Católica do Rio de Janeiro (PUC-Rio), Rio de Janeiro, Brazil, associated with Universidade Federal do Rio de Janeiro (UFRJ), Rio de Janeiro, Brazil*
[60]*Institut für Physik, Universität Rostock, Rostock, Germany, associated with Physikalisches Institut, Ruprecht-Karls-Universität Heidelberg, Heidelberg, Germany*
[61]*National Research Centre Kurchatov Institute, Moscow, Russia, associated with Institute of Theoretical and Experimental Physics (ITEP), Moscow, Russia*
[62]*KVI - University of Groningen, Groningen, The Netherlands, associated with Nikhef National Institute for Subatomic Physics, Amsterdam, Netherlands*
[63]*Celal Bayar University, Manisa, Turkey, associated with European Organization for Nuclear Research (CERN), Geneva, Switzerland*

[a] P.N. Lebedev Physical Institute, Russian Academy of Science (LPI RAS), Moscow, Russia.
[b] Università di Bari, Bari, Italy.
[c] Università di Bologna, Bologna, Italy.
[d] Università di Cagliari, Cagliari, Italy.
[e] Università di Ferrara, Ferrara, Italy.
[f] Università di Firenze, Firenze, Italy.
[g] Università di Urbino, Urbino, Italy.
[h] Università di Modena e Reggio Emilia, Modena, Italy.
[i] Università di Genova, Genova, Italy.
[j] Università di Milano Bicocca, Milano, Italy.
[k] Università di Roma Tor Vergata, Roma, Italy.
[l] Università di Roma La Sapienza, Roma, Italy.
[m] Università della Basilicata, Potenza, Italy.
[n] AGH - University of Science and Technology, Faculty of Computer Science, Electronics and Telecommunications, Kraków, Poland.
[o] LIFAELS, La Salle, Universitat Ramon Llull, Barcelona, Spain.
[p] Hanoi University of Science, Hanoi, Viet Nam.
[q] Università di Padova, Padova, Italy.
[r] Università di Pisa, Pisa, Italy.
[s] Scuola Normale Superiore, Pisa, Italy.